EUROCODE 3-BASED FEA OPTIMIZATION OF TRIANGULAR LIFTING PLATES

[1]Nawajish Ali, [2] Dr. Subbarao Chamarthi,

[1]M-Tech Student, [2]Associate Professor
[1]Mechanical Engineering,
[1]Lingaya's Vidyapeeth, Faridabad, India

Abstract: Lifting plates are critical components in industrial material handling, where structural failure can lead to severe safety hazards and operational losses. Despite their widespread use, the design of triangular lifting plates often lacks rigorous analytical validation, particularly under internationally recognized standards. This study addresses that gap by presenting a systematic design optimization and finite element analysis (FEA) validation of a triangular lifting plate in compliance with Eurocode 3 (EN 1993). The plate geometry and key dimensional parameters were carefully refined to reduce material consumption while maintaining structural performance within acceptable stress and deformation limits. FEA simulations were conducted to examine von Mises stress distribution, total deformation, and factor of safety under realistic loading conditions. The computed results were benchmarked against Eurocode 3 provisions, confirming full structural compliance. The optimized design achieved a notable reduction in weight without sacrificing integrity, making it a practical and economical solution for lifting applications. These findings offer practicing engineers a dependable and code-compliant design framework for developing and certifying triangular lifting plate components in real-world industrial settings.

Index Terms - Below-the-hook lifting device; EN 1993-1-8; pin connection; weight optimization; finite element analysis; S355 steel; von Mises stress; Eurocode 3; bearing resistance; dynamic amplification factor.

1.0 LITRATURE REVIEW

Lifting devices are critical components in industrial material handling, construction, and offshore operations, where structural failure can result in severe consequences including loss of life and equipment damage. Below-the-hook (BTH) lifting devices, such as lifting plates and spreader beams, are widely used to transfer loads between the crane hook and the suspended object. Among these, triangular pin-connected lifting plates offer a simple, lightweight, and cost-effective solution for symmetrical load distribution. Despite their widespread application, the structural design of such devices remains governed by conservative analytical approaches that frequently result in overdesigned and unnecessarily heavy components. Current design practice for pin-connected lifting devices is governed by EN 1993-1-8:2005 in Europe and ASME BTH-1 in North America. EN 1993-1-8 Table 3.9 prescribes minimum geometrical requirements for pin-ended members, including edge distance and bearing resistance criteria, ensuring adequate load transfer at pin interfaces. However, these code provisions are inherently conservative and do not account for the full stress redistribution capacity of the plate, which can only be captured through advanced numerical methods such as finite element analysis (FEA). The safe and efficient lifting of heavy loads is a critical operation in industries ranging from construction and energy to logistics and manufacturing. When it comes to overhead lifting. operations, correct specification and the use of appropriate standards are clearly only part of the story combined with an equally professional approach to issues such as planning, supervision and training, they can undoubtedly go a long way to both reducing the risk of accidents and improving the overall efficiency of lifting throughout the steel industry. Cranes are the leading equipment used in material handling because they can perform the task safely and efficiently [1]. The advent of Computer-Aided Engineering (CAE) has revolutionized the design process for lifting equipment, moving it from traditional, often conservative, manual calculations towards optimized, validated digital prototypes. Finite Element Analysis (FEA) is now a cornerstone of this process, allowing for precise prediction of stress distribution, identification of concentration points, and virtual optimization before physical fabrication. This capability is clearly demonstrated in the domain of lifting equipment [2] Material selection also plays a critical role in the design of Lifting plate, with structural steels such as S355 being widely used due to their high strength-to-weight ratio and good weldability, as supported by studies on S355 steel behaviour in structural applications. Other elements commonly associated with spreader beam are hooks, shackles, chokers, and slings. Shackles are used to connect the lines to the lifting plate. Shackles come in various patterns and capacities. The capacities of specific rigging components must be verified as per the requirement, reliability, grade and safety factor. The Crosby Group and Gunnebo Industries catalogues (Imperial Edition, 2025–2026) were used for the selection and specification of rigging components. [3] The fundamental design principles for such equipment, including load calculations and structural configurations, are well-established in foundational literature [4]. EN 13155 encompasses huge range of devices that can be hung from the hook of a crane. These include many that are widely used in the steel industry, such as lifting beam, spreader beam and other non-fixed load lifting attachments. This is the product of several years 'guaranteed standards of safety with sufficient flexibility for manufacturers to produce innovative and cost-effective customized lifting solutions. [5]. Several studies have investigated the structural behaviour of lifting devices under static and dynamic loading conditions. Kang et al. [6] examined stress concentrations in lifting lugs using nonlinear FEA and reported significant deviation from analytically predicted stress fields near pin holes. Duerr [7] provided a comprehensive review of pin connection design provisions under ASME BTH-1, highlighting limitations of simplified analytical models. Terrez et al. [8] demonstrated that topology optimization of below-the-hook devices can yield mass reductions exceeding 40% without compromising structural integrity. Despite these contributions, limited work has systematically integrated Eurocode-based analytical verification, parametric weight optimization, and FEA validation within a unified design workflow for triangular BTH lifting plates. This study addresses this gap by presenting a complete design methodology for a triangular BTH lifting plate rated at 8.5 tonnes safe working load. The baseline geometry is first verified analytically in accordance with EN 1993-1-8:2005 under a

factored design load incorporating a dynamic amplification factor of 1.5 per EN 1991-3. A parametric optimization is subsequently performed, achieving a 47% reduction in plate mass while maintaining full code compliance. Finally, the optimized design is validated through nonlinear FEA incorporating surface-to-surface pin contact and a bilinear isotropic hardening material model for S355 steel. The remainder of this paper is organized as follows: Section 2 describes the analytical formulation, Section 3 presents the optimization methodology, Section 4 details the FEA setup and results, and Section 5 draws conclusions.

2.0 METHODOLOGY

2.1 Material Selection and Properties

The triangular lifting plate was manufactured from EN 10025-2 hot-rolled structural steel grade S355. This grade is widely used in lifting and structural applications due to its combination of high yield strength, good weldability, and favourable toughness at low temperatures. Table 1 summarizes the mechanical and physical properties applied in the ANSYS material model.

Table 1. Mechanical and Physical Properties of S355 Steel

Properties	Symbol	Value	Unit
Young's Modulus	E	210,00	MPa
Poisson's Ratio	ν	0.30	—
Density	ρ	7850	kg/m³
Yield Strength	F_y	355	MPa
Ultimate Tensile Strength	F_u	470-630	MPa
Elongation at Fracture	A	≥ 22	%

S355 offers a 42% higher yield strength compared to S235, enabling meaningful weight savings relative to lower-grade alternatives while maintaining full compliance with EN 10025-2 chemical and mechanical requirements. A linear elastic isotropic material model was adopted for all FEA computations, consistent with the elastic analysis framework prescribed by ASME BTH-1. The triangular lifting plate was designed and modelled in SolidWorks for an 8.5-ton load capacity. Initially, a preliminary design was developed, which was subsequently optimized to improve structural efficiency. The original weight of the lifting plate was **17.6 kg**; after optimization, the weight was reduced to **9.2 kg**, achieving a weight reduction of approximately **47%** without compromising structural integrity. Figure 1 shows the preliminary and optimized 3D conceptual models. Key performance parameters, including von Mises stress, total deformation, safety factor, and strain, were evaluated using ANSYS Workbench. Following the optimization process, the modified design was reanalysed using the same simulation framework. The results obtained before and after optimization were systematically compared to ensure that the reduced-weight design met all required strength and safety criteria.

2.2 Material Optimization of a Lifting Plate.

In the first part of this study, we analysed a solid plate that had no hole or cavity in the centre. The purpose of this initial analysis was to understand how the plate behaves under load and to use these results as a reference point for comparison. Using finite element analysis, we measured the von Mises stresses, total deformation, and plastic strain in the plate. The results showed that the highest stresses were concentrated near the loading point, which is a fairly common observation in such structural components. After understanding the behaviour of the solid plate, we moved on to optimizing its design. To reduce unnecessary material and make the plate more efficient, we removed material from the central region of the plate, as shown in Figure 1. This kind of modification is widely used in structural optimization to reduce weight without significantly affecting the strength of the component. Once the optimized plate was ready, we analysed it again using ANSYS Workbench under the same loading and boundary conditions as before. The results were quite encouraging — the von Mises stress, deformation, and plastic strain values did not change drastically compared to the original solid plate. We did notice some high stress values appearing at locations where the geometry changes suddenly, but these are known as stress singularities and are a common limitation of finite element models at sharp transitions rather than real physical stresses. More importantly, since we are designing this lifting plate under **Service Class 1** as defined by the **ASME BTH-1** standard, the total number of load cycles is expected to be less than **20,000**. Under these conditions, the standard does not require a fatigue analysis to be performed. Therefore, the stress singularities observed at the geometric discontinuities can be safely ignored, and the overall design can be considered structurally acceptable based on the analysis performed.

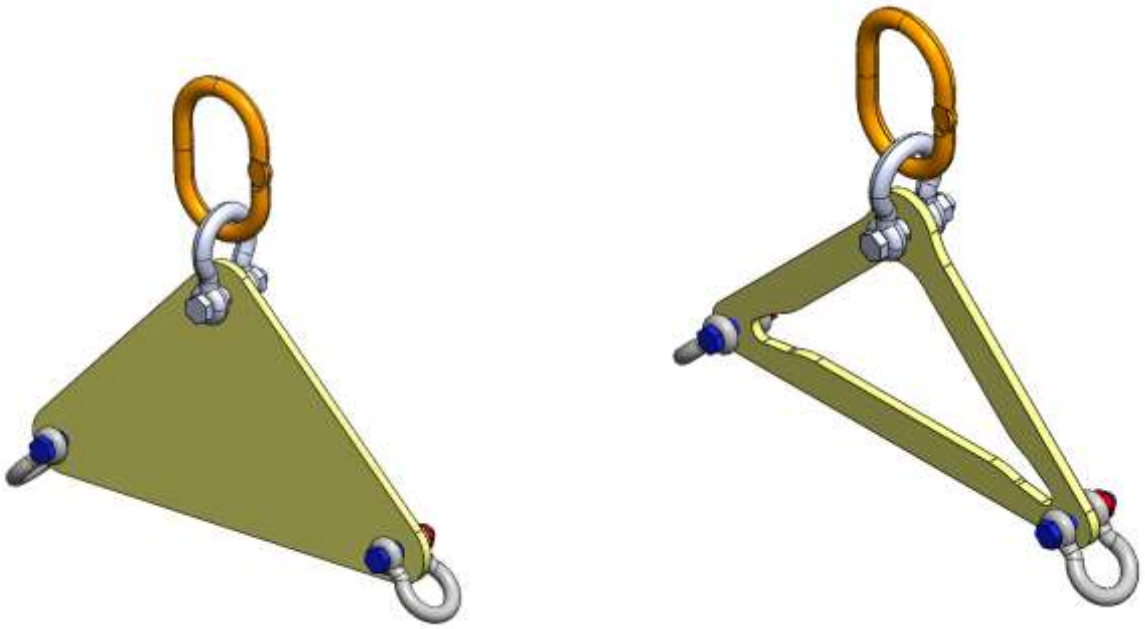

Figure 1: Preliminary and optimized 3D models of the lifting plate.

3.0 Analytical Formulation

This section presents the analytical formulation for the structural verification of a triangular lifting plate used in load-handling operations. The lifting plate is fabricated from S355 structural steel and features one top pin hole for the lifting shackle and two bottom pin holes for the suspended load. The verification is performed in accordance with EN 1993-1-8:2005 (Eurocode 3 — Design of Steel Structures: Design of Joints), specifically Table 3.9 governing geometrical requirements for pin-ended members

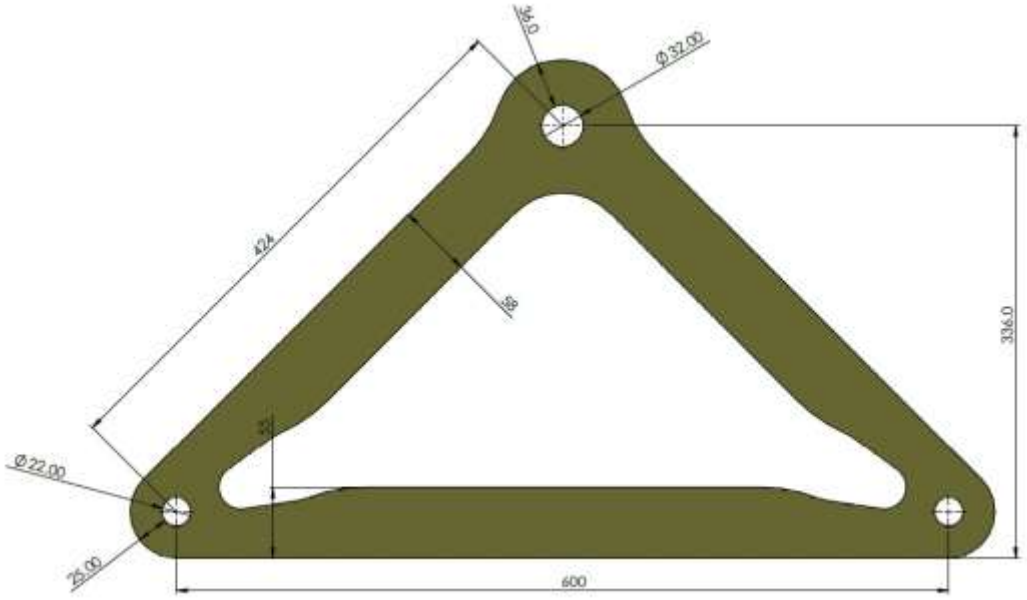

Figure 2: Parametric dimension of optimized lifting plate.

3.1 Design Loading

3.2 Static Load

The safe working load (SWL) is 8.5 tonnes. The equivalent static force is:

$$F_{static} = SWL \times g = 8.5 \times 10^3 \times 9.81 = 83{,}385\ N \approx 83.4\ kN$$

3.3 Dynamic Amplification Factor (DAF)

A dynamic amplification factor (DAF) of **1.5** is applied in accordance with EN 1991-3:2006, Hoisting Class HC3 (moderate hoisting speed). The DAF accounts for dynamic effects arising during the lifting operation, including load swing and impact during pickup. The design load is therefore:

$$F_{Ed} = F_{static} \times DAF = 83.4 \times 1.5 = 125.1\ kN$$

3.4 Analytical Verification

The analytical checks are performed for three failure modes at each pin hole:

(i) Geometrical adequacy of edge distance per Eurocode 3 Table 2,
(ii) Bearing resistance of the pin, and
(iii) Net section tension capacity. Additionally, the diagonal arm member is checked for axial tension.

Table 2. Geometric and Material Input Data

Parameter	Symbol	Value	Unit
Safe Working Load	SWL	8.5	t
Design Load (SWL × 9.81)	Fstatic	83.4	kN
Dynamic Amplification Factor	DAF	1.5	–
Design Force	F_{Ed}	125.1	kN
Plate Thickness	t	15	mm
Yield Strength (S355)	fy	355	MPa
Ultimate Strength (S355)	fu	510	MPa
Partial Factor (resistance)	γ_{M0}	1.0	–
Top Hole Diameter	d_0 (top)	32	mm
Top Hole Edge Distance	a (top)	36	mm
Bottom Hole Diameter	d_0 (bot)	22	mm
Bottom Hole Edge Distance	a (bot)	25	mm
Arm Width at Section	b_arm	58	mm
Arm Length (diagonal)	L_arm	424	mm

3.5 Geometrical Requirements

For pin-ended members of given thickness (Type A), EN 1993-1-8 Table 3.9 stipulates minimum edge distances as follows:

$$a_{min} = F_{Ed}\,\gamma_{M0} / (2 \cdot t \cdot f_y) + (2 \cdot d_0) / 3$$

$$c_{min} = F_{Ed}\ \ \gamma_{M0} / (2 \cdot t \cdot f_y) + d_0 / 3$$

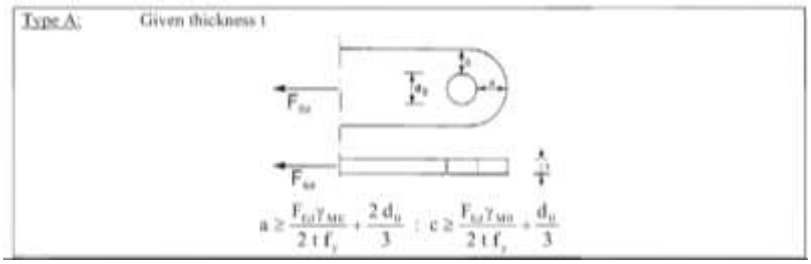

Figure 3: Geometric requirement for pin-based arrangement.

where a is the edge distance in the load direction, d_0 is the hole diameter, t is the plate thickness, and F_{Ed} is the design force at the pin.

3.6 Top Hole (Lifting Point) d_0 = 32 mm, a = 36 mm, F_{Ed} = 125.1 kN

$$a_{min} = 125{,}100 \times 1.0 / (2 \times 15 \times 355) + (2 \times 32) / 3$$

$$a_{min} = 11.8 + 21.3 = 33.1 \text{ mm}$$

Check: a provided = 36 mm ≥ a_{min} = 33.1 mm → PASS ✓

3.7 Bottom Holes (Load Point) - d_0 = 22 mm, a = 25 mm

The total design load is shared equally between the two bottom holes. Each hole carries:

$$F_{Ed,bot} = 125.1 / 2 = 62.55 \text{ kN}$$

$$a_{min} = 62{,}550 \times 1.0 / (2 \times 15 \times 355) + (2 \times 22) / 3$$

$$a\_min = 5.9 + 14.7 = 20.6 \text{ mm}$$

Check: $a_{provided}$ = 25 mm ≥ a_{min} = 20.6 mm → PASS ✓

3.8 Pin Bearing Resistance — Eurocode3 Cl. 3.6.1

The bearing resistance of the plate at the pin hole is checked per Eurocode 3 Cl. 3.6.1(2):

$$F_{b,Rd} = 1.5 \times fy \times d_{pin} \times t / \gamma_{M0}$$

where d_{pin} is the nominal pin diameter, taken as $d_o - 1\ mm$ to account for clearance.

3.9 Top Hole — d_{pin} = 31 mm

$$F_{b,Rd} = 1.5 \times 355 \times 31 \times 15 / 1000 = 247.6 \text{ kN}$$

Check: $F_{b,Rd}$ = 247.6 kN ≥ F_{Ed} = 125.1 kN → PASS ✓

3.10 Bottom Holes -- d_{pin} = 21 mm

$$F_{b,Rd} = 1.5 \times 355 \times 21 \times 15 / 1000 = 167.7 \text{ kN}$$

Check: $F_{b,Rd}$ = 167.7 kN ≥ $F_{Ed,bot}$ = 62.6 kN → PASS ✓

4.11 Net Section Tension Capacity — Eurocode 3 Cl. 6.2.3

The net cross-sectional area at the pin hole is calculated as the area of material remaining on both sides of the hole in the load direction:

$$A_{net} = 2 \times (a - d_o/2) \times t$$

$$F_{net,Rd} = A_{net} \times fy / \gamma_{M0}$$

4.12 Top Hole

$A_{net} = 2 \times (36 - 32/2) \times 15 = 2 \times 20 \times 15 = 600 \text{ mm}^2$

$F_{net,Rd} = 600 \times 355 / 1000 = 213.0 \text{ kN}$

Check: 213.0 kN ≥ 125.1 kN → PASS ✓

4.13 Bottom Holes

$$A_{net} = 2 \times (25 - 22/2) \times 15 = 2 \times 14 \times 15 = 420 \text{ mm}^2$$

$$F_{net,Rd} = 420 \times 355 / 1000 = 149.1 \text{ kN}$$

Check: 149.1 kN ≥ 62.6 kN → PASS ✓

4.14 Diagonal Arm — Axial Tension Capacity

The plate geometry forms a triangle with overall height H = 336 mm, base = 600 mm and diagonal arm length L = 424 mm as per Figure 2. Each diagonal arm carries an axial tension force resolved from the vertical equilibrium at the top pin:

$$F_{\_arm} = (F_{Ed} / 2) \times (L / H) = (125.1 / 2) \times (424 / 336) = 78.9\ kN$$

The gross cross-sectional area of the arm at the critical section (width = 58 mm, thickness = 15 mm):

$$A_{gross} = 58 \times 15 = 870\ mm^2$$

$$F_{\_t,Rd} = A_{gross} \times fy / \gamma_{M0} = 870 \times 355 / 1000 = 308.9\ kN$$

Check: 308.9 kN ≥ 78.9 kN → PASS ✓

4.15 Summary of Results

Table 2 summarizes the results of all structural checks performed on the triangular lifting plate. All checks satisfy the requirements of EN 1993-1-8.

Table 3 — Summary of Verification Checks

Check Description	Capacity	Allowed	Status
Top hole – Edge distance	36.0 mm	33.1 mm req.	**PASS** ✓
Top hole – Bearing resistance	247.6 kN	125.1 kN	**PASS** ✓
Top hole – Net section tension	213.0 kN	125.1 kN	**PASS** ✓
Bottom hole – Edge distance	25.0 mm	20.6 mm req.	**PASS** ✓
Bottom hole – Bearing resistance	167.7 kN	62.6 kN	**PASS** ✓
Bottom hole – Net section tension	149.1 kN	62.6 kN	**PASS** ✓
Diagonal arm – Tension capacity	308.9 kN	78.9 kN	**PASS** ✓

3.0 FEA SETUP AND RESULTS-

Finite Element Analysis (FEA) was carried out using ANSYS Workbench to evaluate the structural performance of the plate under prescribed loading and boundary conditions. The analysis was performed using a static structural solver, assuming linear elastic material behaviour. The material properties assigned to the plate were isotropic, with Young's modulus, Poisson's ratio, and yield strength defined according to standard structural steel specifications. The geometry was imported into the ANSYS Mechanical environment, where appropriate boundary conditions and loads were applied to simulate realistic operating conditions. A mesh convergence study was conducted to ensure the accuracy and reliability of the results. Based on this study, an optimal mesh size was selected to balance computational efficiency and solution accuracy.

3.1 Plate Analyzed without the cavity. (Case 1)

In the first case, the plate was analyzed without any geometric optimization (i.e., without introducing a cavity) to establish a baseline for structural performance. This initial analysis helps in understanding the stress distribution, deformation characteristics, and load-carrying behavior of the original design. The results obtained from this case are illustrated in Figures 4 to 7 and Table 4.

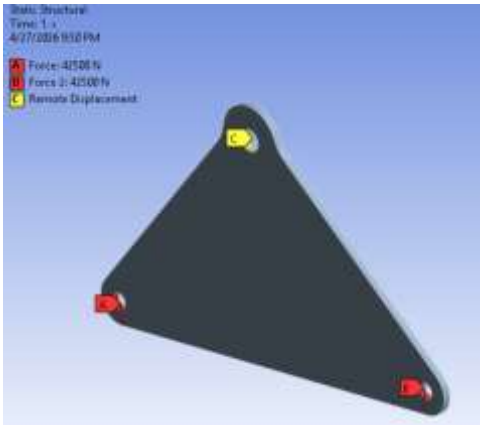

Figure 4: Boundary condition

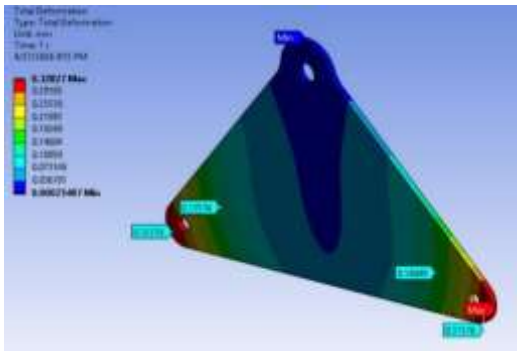

Figure 5: Total deformation

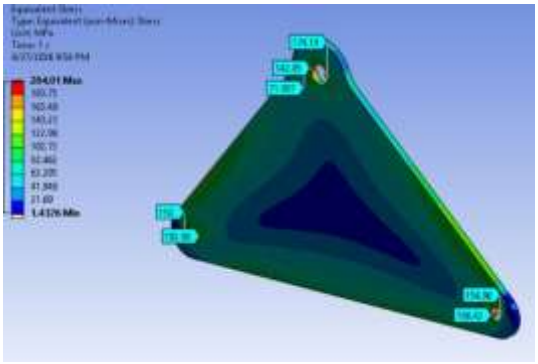

Figure 6: Von mises stress

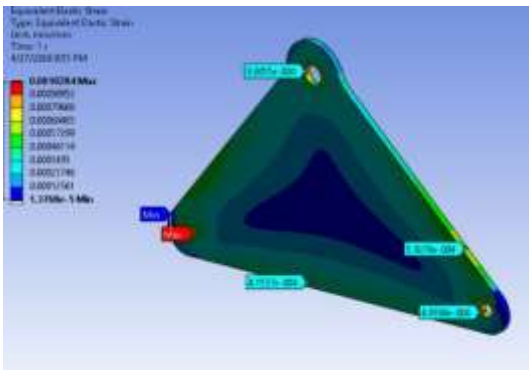

Figure 7: Plastic strain

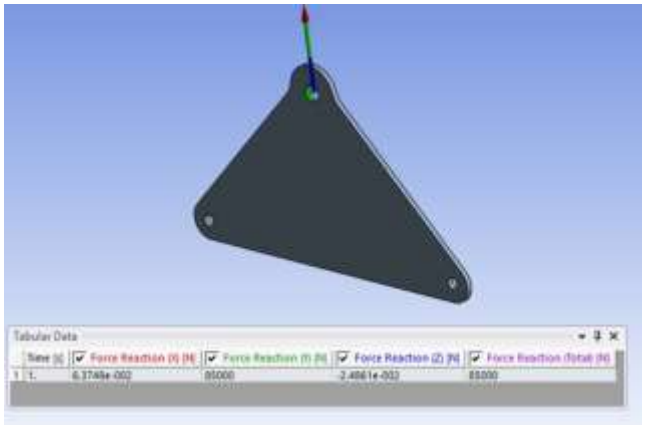

Figure 8: Force Reaction

Table 4 — FEA result case 1

Parameter	Value	Unit
Force Applied	8500 (total)	Newton
Von mises stresses	204	Mpa
Deformation	0.32	mm
Plastic strain	.00102	--
Reaction force	8500	Newton
Weight of Plate	17.6	kg
Cost of plate	30	Euro

3.2 Optimized plate Analyzed with FEA (Case 2)

In this case, the plate was analysed after geometric optimization by introducing a cavity. This was done to evaluate the structural behaviour of the optimized design and to compare its performance with the unoptimized plate. The analysis was carried out under the same boundary conditions, loading, and solver settings as defined in Case 1 to ensure consistency in results. The mesh was refined near the cavity region to accurately capture stress concentrations and deformation behaviour. This analysis helps in understanding the effect of material removal on stress distribution, deformation, and overall structural efficiency of the plate. The results obtained for the optimized plate are shown in **Figures 7 to 12**. and Table 5.

Figure 8: Boundary condition

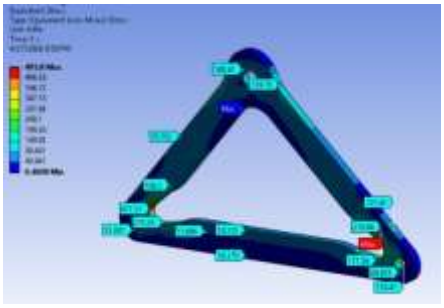

Figure 9: Von mises stresses

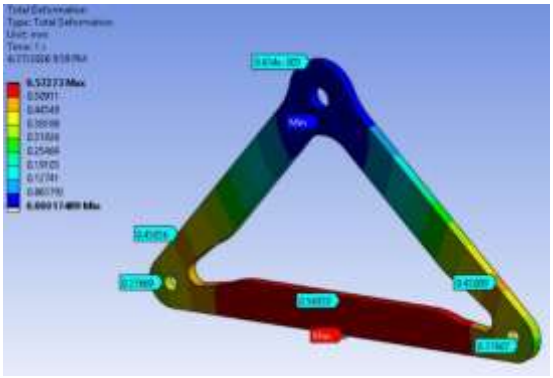

Figure 10: Total deformation

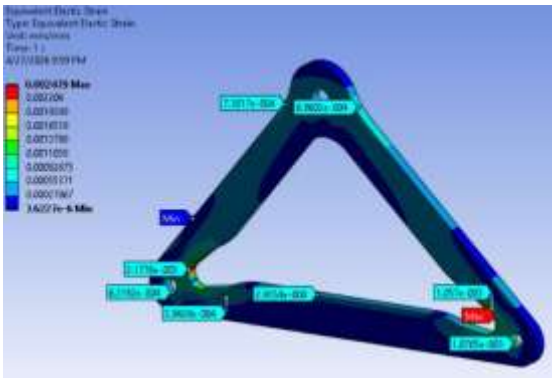

Figure 11: Plastic strain

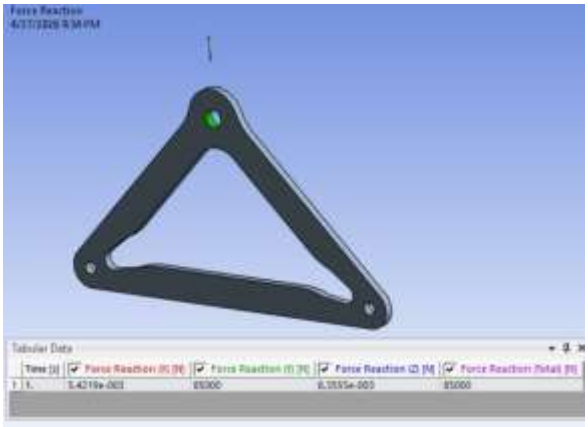

Figure 12: Reaction Force

Table 5 — FEA result case 2

Parameter	**Value**	**Unit**
Force Applied	8500 (total)	Newton
Von mises stresses	495	Mpa
Deformation	0.52	mm
Plastic strain	.00247	--
Reaction force	8500	Newton
Weight of Lifting plate	9.2 kg	kg
Cost	17	Euro

4.0 RESULTS AND DISCUSSION

A comprehensive comparison was carried out between the unoptimized plate (Case 1) and the optimized plate with cavity (Case 2) under identical loading conditions of **8500 N**. The optimized design achieved a significant reduction in weight from **17.6 kg to 9.2 kg**, corresponding to approximately **47.7% reduction**, along with a cost reduction from **30 Euro to 17 Euro** (≈ **43.3% savings**),

demonstrating clear economic and material efficiency. However, the reduction in material resulted in increased stress and deformation. The maximum von Mises stress increased from **204 MPa** in Case 1 to **495 MPa** in Case 2, representing an increase of approximately **142.6%**. This rise in stress is primarily attributed to localized stress concentration effects near the cavity edges due to geometric discontinuities. These peak stresses are confined to small regions and are mesh-sensitive in nature. Since the present study focuses on static structural analysis and does not consider fatigue loading, such localized stress concentrations may be considered acceptable provided they do not govern overall structural failure or excessive plastic deformation. The total deformation increased from **0.32 mm to 0.52 mm** (≈ **62.5% increase**), indicating a reduction in stiffness due to material removal. Similarly, the plastic strain increased from **0.00102 to 0.00247**, suggesting localized yielding in the optimized configuration. The reaction force remained constant at **8500 N** in both cases, confirming the consistency of boundary conditions and load application. Overall, the optimized plate demonstrates a highly efficient design in terms of weight and cost reduction, albeit with increased stress and deformation. The design can be considered structurally viable if the induced stresses remain within the allowable limits of the selected material. Nevertheless, further geometric refinement, such as the introduction of fillets or smooth transitions around the cavity, is recommended to mitigate stress concentrations and enhance structural performance. Figure 12 represent the line diagram of comparison von mises stresses, total deformation and plastic strain Figure 13 compare the weight and cost and table 6 illustrated comparison of all other parameter in case 1 and case 2 .

Table 6 — Comparison Table case 1 and case 2

Parameter	**Value in case 1**	**Value in case 1**	**Unit**
Force Applied	8500 (total)	8500 (total)	Newton
Von mises stresses	204	495	Mpa
Deformation	0.32	0.52	mm
Plastic strain	.00102	.00247	--
Reaction force	8500	8500	Newton
Weight of Lifting plate	17.6	9.2	kg
Cost	30	17	Euro

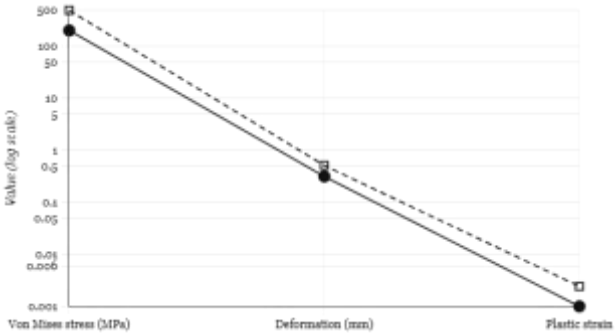

Figure 12: Line diagram of stresses, deformation and strain for both the cases.

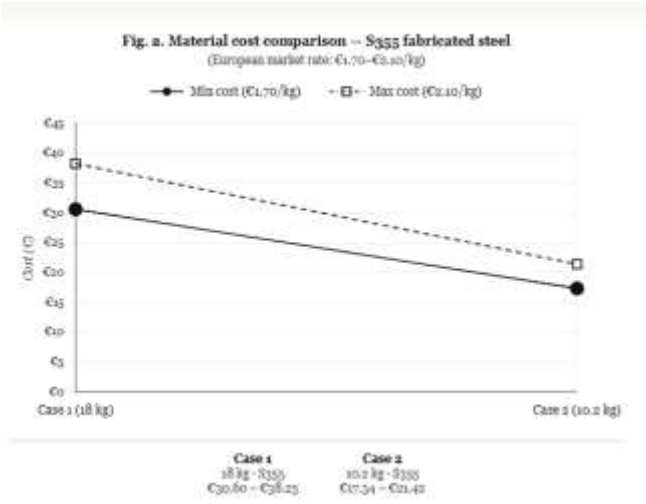

Figure 13: Cost comparison for both the cases.

5.0 CONCLUSION

In this study, a structural analysis of a lifting plate was carried out using Finite Element Analysis (FEA) to evaluate the effectiveness of geometric optimization through cavity introduction. Two cases were considered: an unoptimized plate (Case 1) and an optimized plate with a cavity (Case 2), both subjected to identical loading and boundary conditions. The optimized design demonstrated a significant **weight reduction of approximately 47.7%** and a corresponding **cost reduction of 43.3%**, highlighting its potential for material and economic efficiency. However, this reduction in mass resulted in increased structural response, with the maximum

von Mises stress rising by approximately **142.6%** and total deformation increasing by **62.5%** compared to the unoptimized configuration. The peak stresses observed in the optimized plate were found to be localized around the cavity edges due to stress concentration effects. Since the present work focuses on static loading conditions, these localized stresses may be considered acceptable if they do not govern overall structural failure and remain within permissible material limits. Nevertheless, the increase in plastic strain indicates the onset of localized yielding, which should be carefully evaluated in practical applications. Overall, the study demonstrates that cavity-based optimization is an effective approach for achieving substantial weight reduction in lifting components. However, it also highlights the trade-off between weight savings and structural performance. For safe and efficient design, it is recommended to refine the cavity geometry by incorporating smooth transitions or fillets and, if necessary, to utilize higher strength materials to ensure that stress levels remain within allowable limits.This work provides a foundation for further research in structural optimization, including fatigue analysis, advanced topology optimization techniques, and compliance with design standards such as Eurocode or ASME for real-world applications.

REFERENCES

[1] V. Herrera-Perez, F. Salguero-Caparros, M. d. C. Pardo- Ferreira, and J. C. Rubio-Romero, ″Key factors in crane-related occupational accidents in the Spanish construction industry (2012–2021),″ International journal of environmental research and public health, vol. 20, no. 22, p. 7080, 2023

[2] A. Andras, F. D. Popescu, S. M. Radu, D. Pasculescu, I. Brinas, M. A. Radu, and D. Peagu, ″Numerical simulation and modeling of mechano–electro–thermal behaviour of electrical contact using comsol multiphysics,″ Applied Sciences, vol. 14, no. 10, p. 4026, 2024.

[3] ″Crosby and Gunnebo industries catalogue – imperial 2025-2026.,″

[4] M. Kohler, S. Jenne, K. Potter, and H. Zenner, "Load assumption for fatigue design of structures and components," Springer. doi, vol. 10, pp. 978–3, 2017.

[5] ″European committee for standardization. en 13155: Cranes — safety — non-fixed load lifting attachments. Brussels: Cen, 2020,″

[6] B.-S. Kang, G. J. Park, and J. S. Arora, ″Optimization of flexible multibody dynamic systems using the equivalent static load method,″ AIAA journal, vol. 43, no. 4, pp. 846–852, 2005.

[7] D. Duerr, ″Design factors for fabricated steel belowthe-hook lifting devices,″ Practice Periodical on Structural Design and Construction, vol. 13, no. 2, pp. 48–52, 2008.

[8] F. B. MARIN, D. L. BURUIANAˇ , L. IONICAˇ , and M. MARIN, "Topology optimization for mass reduction of a structural component in a surgical robotic arm," The Annals of "Dunarea de Jos" University of Galati. Fascicle IX, Metallurgy and Materials Science, vol. 48,no. 4, pp. 51–56, 2025.